Measurement of the elastic modulus of homogeneous materials by a bending wave speed method

Antonio Esposito, Jonathan Hargreaves, Rosario Romano, Andrea Cicero

MEASUREMENT OF THE ELASTIC MODULUS OF HOMOGENEOUS MATERIALS BY A BENDING WAVE SPEED METHOD

Antonio Esposito[1] Jonathan A. Hargreaves[2] Rosario A. Romano[1] Andrea Cicero[3]
[1]Department of Industrial Engineering, University of Naples Federico II, Italy
[2]Acoustics Research Group, University of Salford, UK
[3]Eupro Srl, Via del Fante 8, 97100 Ragusa, Italy
antonio.esposito8@unina.it

ABSTRACT

Elastic modulus is one of the most important mechanical properties of homogeneous materials. It describes the dynamic behaviour of elastic and viscoelastic materials, strongly affecting both panel modes and coincidence frequencies, so is an important quantity to consider in noise and vibration control. A method to obtain the elastic modulus of materials is proposed herein, based on the measurement of the surface velocity field occurring due to the propagation of bending waves through a panel. A 2D spatial Fourier transform applied to the measured velocity field allowed evaluation of the wavevectors of the free bending waves propagating in the panel. By averaging over wave direction, the overall amplitude distribution versus wavenumber can be found, and from this the dominant wavenumber obtained. From the latter it is straightforward to calculate the flexural wave speed, which can, via classical plate theory, be related to the static elastic modulus value of the material. A preliminary experimental test-rig was based on laser Doppler vibrometry measurements in order to assess the surface velocity of a freely suspended sample, acoustically excited by a broadband signal. The experimental results show a reasonable agreement to the manufacturer's technical data and to the outcomes of related numerical simulations, although some issues require further research.

1. INTRODUCTION

Propagation of vibrational waves in homogeneous plates is a topic that has received substantial study and is well understood [1-2]. In practical applications however, there is often uncertainty over material parameters, for composites in particular, and it is commonplace to observe mismatch between the behaviour of real structures and that predicted by computer models. This is undesirable since it means that designs may not perform as expected. It also challenges the emerging 'Digital Twin' vision. In this, products are accompanied by a tightly aligned digital model that can be used as a performance benchmark. For this to work, both simulation algorithms and material data must be accurate, hence there is a need for accurate material characterisation methods. This is particularly challenging for existing structures that cannot be dismantled and must be characterised in-situ. Here we propose such a technique for measuring bending wave speed and, from this, the elastic modulus. Notably, this method is non-contact and relies upon passive excitation.

Techniques for measuring elastic modulus include static and/or dynamic testing [3], nanoindentation and methods based on measuring speed of bending wave propagation [4-7]. This latter category is non-destructive in its approach, so aligns with the objective of this study. Most have however required attachment of shakers and/or accelerometers; the method proposed here prevents this by passive acoustic excitation and laser Doppler vibrometry. This avoids mass loading, so is applicable for lightweight structures, and ensures that the structure is not damaged.

Methods for measuring panel bending wave speed can be categorised into those based on transient analysis and those using spatial wave decomposition. The former approximates an infinite plate by time-windowing out reflections [6]. This is effective but inevitably limits low frequency accuracy. Spatial decomposition approaches can be applied in one [8] or two [9-10] spatial dimensions, i.e. to bars or plates, and are able to simultaneously extract wavespeeds for different propagation modes and/or different directions, potentially allowing characterisation of orthotropic panels. They have often been applied at high and/or ultrasonic frequencies by the Non-Destructive Testing (NDT) community [11]. The starting point for spatial decomposition methods is usually a spatial Fourier transform. This requires a high-density of measurement points, something that is tedious to acquire with accelerometers but relatively unproblematic with a scanning laser vibrometer. Limitations include: finite aperture effects; an assumption that constituent plane waves are homogeneous (no propagation loss); poor convergence near driving points (due to the cylindrical nature of the vibration field). Recent works have attempted to overcome these limitations by including propagation loss [12-13] and/or source functions [14], or more sophisticated signal processing techniques [15].

In the preliminary test case reported herein, number of scanning points was not a limiting factor hence a 2D Fourier transform could be applied without significant windowing issues. It is also anticipated that distributed acoustic excitation will not infringe the homogeneous plane wave assumption of the Fourier transform so much as for point excitation. The study herein limits itself to

isotropic panels. This allows a new postprocessing step that searches for energy peaks in any propagation direction. This means that instead of struggling to distinguish overlapping modes, as some works above try to do, all modes contribute to the estimate.

2. THEORY

2.1 Plate bending wave theory

It is well known that bending waves in plates are dispersive, that is their wavespeed varies with frequency. According to classical plate theory [1]:

$$c(f) = \sqrt[4]{\frac{Eh^2}{12\rho(1-\nu^2)}} \times \sqrt{2\pi f}. \quad (1)$$

Here:

- E is the elastic modulus of the material (Nm^{-2})
- h is the thickness of the plate (m)
- ρ is the mass density of the material (kgm^{-3})
- ν is the Poisson ratio of the material

Noting that wavenumber $k = 2\pi f/c$ gives:

$$k(f) = \sqrt[4]{\frac{12\rho(1-\nu^2)}{Eh^2}} \times \sqrt{2\pi f}. \quad (2)$$

It is therefore expected that k will follow a $\sqrt{f}$ trend. The method estimates E by fitting a curve $k(f) = m\sqrt{f}$ to measured wavenumber data and then using:

$$E = 48\pi^2\rho(1-\nu^2)/h^2m^4. \quad (3)$$

Regarding the other quantities in Eqn. (3), h can usually be measured and ρ is typically known with good confidence for most materials. Knowledge of ν may be less certain for some materials e.g. composites, though the form of Eqn. (3) means the estimate of E will be relatively insensitive to it for small values at least. It is also worth noting that in many numerical models, e.g. FEM with Mindlin-Reissner shell physics, these parameters are recombined similarly to Eqn. (1), reducing the influence of chosen values.

2.2 Processing by two-dimensional Fourier transform

The data processing method utilised herein builds on the concepts introduced in [9]. A Cross-Power Spectral Density analyser is first used to find the amplitude and phase relationship $v(x,y)$ between out-of-plane velocity, as measured by the laser vibrometer at coordinates (x,y) on the plate, and some reference signal. $v(x,y)$ is sampled at a grid of measurements points, then a two-dimensional Fourier transform converts these spatial measurements into an equivalent wavenumber spectrum $V(k_x,k_y)$:

$$V(k_\mathrm{x},k_\mathrm{y}) = \iint v(x,y)w(x,y)e^{-\mathrm{i}(k_\mathrm{x}x+k_\mathrm{y}y)}dxdy. \quad (4)$$

Here k_x and k_y are wavenumber in the x and y directions respectively. $w(x,y)$ is a spatial window function, a future development recommended by Ferguson et al in [9]. Here it was chosen to be a Hanning window with support over the plate dimensions $0 \le x \le L_x$ and $0 \le y \le L_y$. They also discuss how a Discrete Fourier Transform (DFT) gives insufficient points in $k_\mathrm{x}, k_\mathrm{y}$ space and advocate evaluation of values in-between what a direct 2D Fourier series would deliver. Here that is achieved using the DFT algorithm simply by zero-padding the measured data.

Many of the papers cited in the previous section have the aim of characterising angle-dependent wave speed for orthotropic plates. Here the scope has been limited to isotropic plates, offering an advantage in how dominant wavenumber can be estimated. Rather than searching for peaks in k_x, k_y space, and struggling with distinguishing between overlapping modes, we consider that any mode for a rectangular plate will be built out of plane waves with a bending wavenumber matching that frequency. All such modes can then contribute to the estimate of wavenumber at that frequency, regardless of direction or phase.

$Q(k)$ is introduced as a measure of power in wavenumber $k = \sqrt{k_\mathrm{x}^2 + k_\mathrm{y}^2}$, regardless of direction. It is defined as:

$$Q(k) = \int_0^{2\pi} k|V(k\cos\theta, k\sin\theta)|^2 d\theta. \quad (5)$$

Here θ is propagation angle so $k_\mathrm{x} = k\cos\theta$ and $k_\mathrm{y} = k\sin\theta$. It is related to total power by:

$$\iint |V(k_\mathrm{x},k_\mathrm{y})|^2 dk_\mathrm{x}dk_\mathrm{y} = \int_0^\infty Q(k)dk. \quad (6)$$

$Q(k)$ is expected to have peak at the bending wavenumber for the material. A peak-search at each frequency should therefore give $k(f)$, and from this E via Eqn. (3). Q will experience peak-widening due to the spatial window present in Eqn. (4), but this will be symmetrical so peak location should be retained.

3. METHOD VALIDATION

The method was tested on an acrylic panel by means of acoustic measurements carried out in the acoustics laboratories at the University of Salford. The post-processing chain was validated by means of numerical simulations performed at the University of Naples.

3.1 Numerical test-case

A three-dimensional vibroacoustic FEM simulation was carried out in COMSOL™ by modelling an acrylic plate in unconstrained conditions, having dimensions 960 mm × 510 mm × 2 mm, acoustically excited by a monopole source in free field. The panel surface velocity field was numerically evaluated and then post-processed by applying the method described in the previous section. The panel was modelled as a linear elastic and isotropic shell, free at the edges, the mechanical properties of

which are defined in Tab. 1. The structural domain was surrounded by a spherical acoustic domain, in which a monopole sound source was defined and located at 3 cm distance from the panel, close to a corner, in order to obtain the highest structural modal density. The exterior boundaries of the spherical air volume were modelled as a Perfectly Matched Layer (PML), in order to approximate free field conditions (Fig.1). The acoustical and mechanical physics were then coupled by means of the 'multiphysics' node, so as to include both the air load on the panel and the structural acceleration experienced by the fluid [16]. Structural and acoustic domains were discretized by means of unstructured tetrahedral meshes ranging from 0.01 m to 0.11 m, and unstructured quadrilateral meshes were used for the PML. As a result of a stationary frequency domain study, complex values of transverse surface velocity were evaluated at a regular grid of 527 (31×17) evenly spaced point receivers distributed over the entire surface of the panel. The spatial periodicity of bending wave propagation at each frequency can be analysed by observing the function $V(k_x, k_y)$ in the wavenumber space. An example at 102 Hz is shown in Fig. 2, where the yellow peaks indicate the dominant wavenumbers. The values of k_x and k_y at the peaks can be related to the number of repetitions of the modes shape in the x and y directions. It can also be seen that while many peaks are present, most have the same value of k, following a circular locus. A peak search on $Q(k)$ will find the radius of this locus.

$Q(k)$ was calculated at each frequency using Eqn. (5). Fig. 3 shows a measure of the vibrational power of bending waves at 102 Hz regardless of propagation direction; the dominant wavenumber k can be then identified as the abscissa corresponding to the peak value of $Q(k)$. By repeating such an operation of peak finding for all frequencies, the wavenumber spectrum $k(f)$ was evaluated (Fig. 4). This shows a trend increasing in frequency with $\sqrt{f}$, as expected from Eqn. (2). From this, the phase velocity spectrum $c(f)$ was calculated (Fig. 5). The slope of a linear fit performed over the entire spectrum of $c(\sqrt{f})$ (also shown) allows to calculate the elastic modulus E according to Eqn. (3). The latter was found to be equal to 3.38 GPa, within 5% of the value set in the FEM model (Tab. 1).

Mass density ρ (kgm^{-3})	1190
Poisson's ratio ν	0.35
Input Young's Modulus E (GPa)	3.2

Table 1. Acrylic plastic mechanical properties, as defined in the COMSOL™ built-in material library.

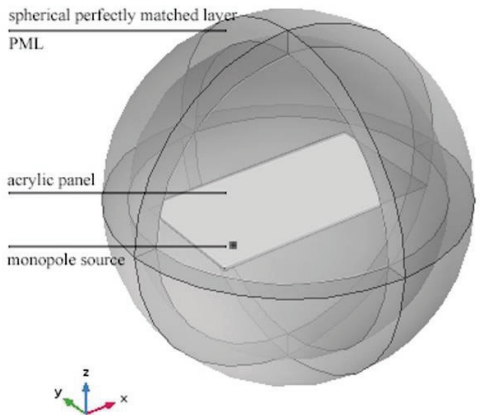

Figure 1. Geometry of the FEM vibroacoustic model. The acoustical domain surrounding the shell is bounded by a spherical Perfectly Matched Layer (PML).

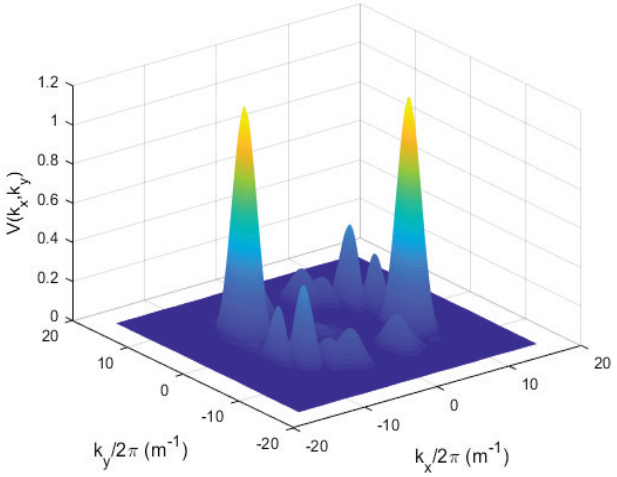

Figure 2. 2D spatial Fourier transform of surface plate velocity field $v(x, y)$ evaluated at 102 Hz.

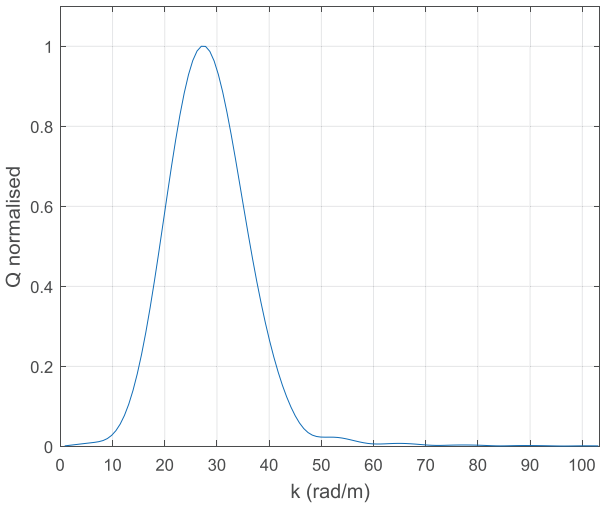

Figure 3. $Q(k)$, the distribution of vibrational energy versus wavenumber, at 102 Hz, normalised to its peak.

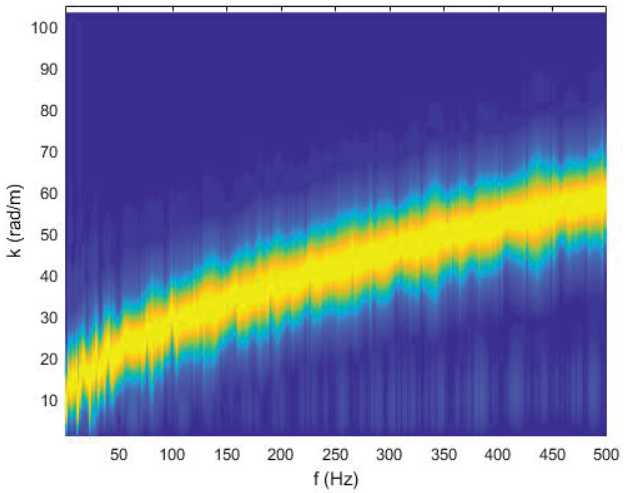

Figure 4. Plot of normalised $Q(k)$ versus wavenumber and frequency. The yellow peak indicates the trend of the numerical dominant wavenumber $k(f)$.

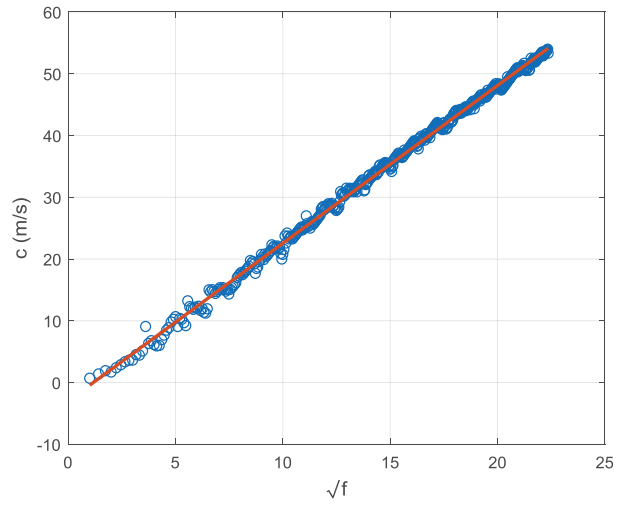

Figure 5. Linear fit of phase speed spectrum: ○ numerical values of $c(\sqrt{f})$, ——— fitting line $y = 2.6\sqrt{f} - 2.9$.

4. MEASUREMENTS OF AN ACRYLIC PLATE

The method was experimentally evaluated by acoustical tests on a rectangular acrylic panel of dimensions 960 mm × 510 mm × 2 mm, as was simulated in FEM in section 3. The acrylic rectangular plate tested in the acoustical measurements was suspended limply from a supporting frame (Fig. 6a), in order to approximate the free edge boundary condition. The panel was excited by a broadband signal, emitted by a loudspeaker placed at its rear. A block diagram is given in Fig. 6b.

As in the numerical case, a scanning grid of 527 evenly spaced points (31×17) was set. A secondary non-scanning LDV, pointing to a fixed position upon the panel, was used as a phase reference. Both had a standoff distance of 1.32 m from the panel. The normal surface velocity field $v(x, y)$ was measured up to 500 Hz with a frequency resolution of 1.25 Hz. $V(k_x, k_y)$ and $Q(k)$ functions were derived according to Eqns. (4) and (5), allowing the dominant wavenumber $k(f)$ to be found.

Fig. 7a shows measured $Q(k)$ versus wavenumber and frequency. As a reference, a black dashed curve is overlaid on the plot, showing the expected trend of the wavenumber calculated according to Eqn. (2) using the reference value of E provided in the technical datasheet (Tab. 2). A match between the two curves is observable up to 300 Hz, above which some outliers are present. Most of these follow a nearly linear trend below 20 rad/m. As suggested by previous work [11], such a linear trend in measured wavenumber might be attributable to the first symmetrical Lamb wave mode S_0 [2]. In order to exclude the outlying values from the post-processing, a high-pass filter was applied to $Q(k)$. The cut-off frequencies of this a filter (red dashed curve) increase in frequency with a factor of $\sqrt{f}$ and were defined by shifting the curve of the expected wavenumber down of 15 rad/m. This produced the plot of $Q(k)$ in Fig. 7b, the peak of which better approximates the expected trend over the entire frequency range, although some noise is still present especially in the interval of 250-400 Hz. Starting from these data, the phase speed spectrum $c(\sqrt{f})$ was calculated and a linear fit performed over the 50-500 Hz frequency interval. The

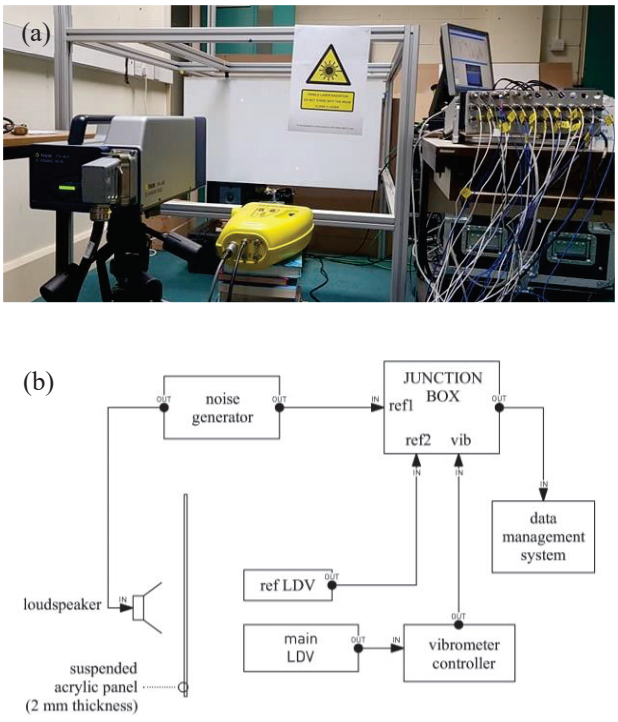

Figure 6. (a) The measurement setup, showing the acrylic panel, supporting frame, and the pair of LDV. The loudspeaker (not visible) is located behind the panel. (b) Block diagram of the measurement setup: output signals from secondary LDV and noise generator were used as references.

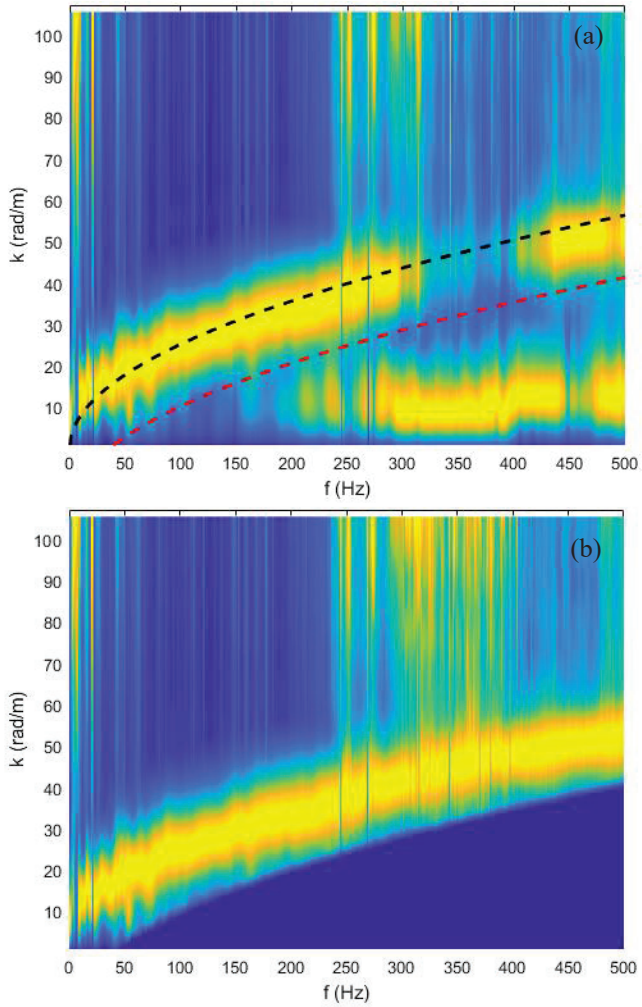

Figure 7. Plot of measured $Q(k)$ versus wavenumber and frequency. (a) normalised unfiltered values where – – – is bending wavenumber trend expected for Young's Modulus reference value $E = 3\ GPa$, and – – – is high-pass filter cut-off frequency. (b) $Q(k)$ high pass filtered following red line in (a), and re-normalised.

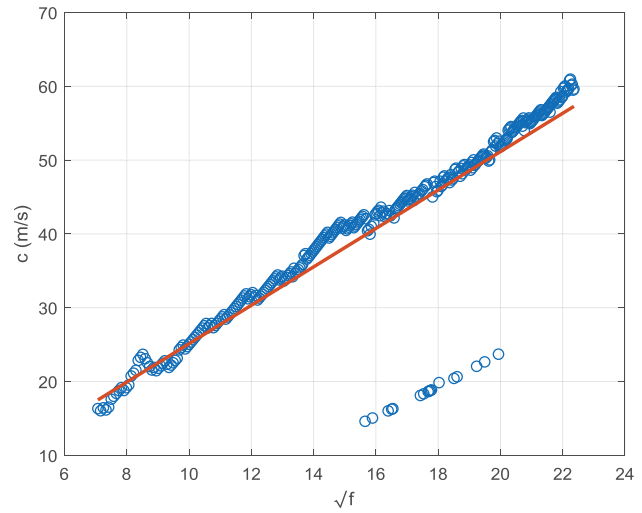

Figure 8. Linear regression of phase speed over the 50-500 Hz frequency range: ○ measured values of $c(\sqrt{f})$, ——— fitting line $y = 2.6\sqrt{f} - 0.9$.

static elastic modulus was then found to be equal to 3.54 GPa, showing a reasonably good match (18% error) with the Young's modulus minimum value of 3.00 GPa reported in the manufacturer's technical datasheet (Tab. 2). The accuracy of this reference data is however also uncertain.

Young's modulus (GPa) (technical datasheet)	Young's modulus (GPa) (proposed method)
3.00 (minimum)	3.54

Table 2. Comparison between elastic modulus reported by IRPEN Policril technical datasheet and the one calculated with the presented method.

5. PRELIMINARY EXTENSION TO NON-HOMOGENEOUS MATERIALS

A preliminary investigation into the applicability of this method for non-homogeneous materials has also been made. The measurement process described in section 4 was repeated on a panel of 'foamcore' (or 'foamboard'), a material which is commonly used as support for photographic prints or architectural scale models. A panel of foamcore is made up of a sandwich structure, which core is polystyrene foam clad with a layer of paper facing on either side, providing a significant structural stiffness when compared to foam as standalone (Fig. 9).

Unfortunately, the obtained data resulted to be much noisier than to those measured on the acrylic sheet, providing low levels of confidence for the evaluation of the elastic modulus. This might be attributed to the more complex structure of the material, which introduces a sensible deviation from the assumption of isotropic and homogeneous material. Moreover, it may also be assumed that a greater internal damping of foamcore has affected the modal behaviour of the sample, leading to low levels of signal-to-noise ratio for the dominant wavenumber to be captured by the LDV. This suggests that improvement is

Figure 9. Example of foamboard sheets, showing the sandwich structure with inner polystyrene foam core and two outer layers of paper (source: www.indiamart.com).

needed in order to extend the method as well as to non-homogeneous materials.

6. CONCLUSIONS

The method for the determination of the elasticity modulus presented in this paper has been shown to work for homogeneous and isotropic materials, providing a good correlation of the obtained values against numerical simulations and manufacturer's data.

This method offers the advantage of being non-destructive on the material under test, as well as of not requiring the use of any mean of excitation or attached sensors such as shakers and piezoelectric accelerometers. In such a manner, any additional loading upon the sample is minimised leaving unaltered its mass and stiffness, therefore avoiding interference on the vibrational field and facilitating the in-situ characterization of lightweight structural elements.

With regards to data acquisition and processing, developments will be implemented on the automatic selection of k windowing and optimised frequency ranges for the linear regression of wave speed values.

Further experimental work includes analysis of the outlier trend seen in Fig. 7a, with the aims to investigate the possible cause and extract any extra data it might offer.

Finally, future investigation should validate and update the method for the analysis of non-homogeneous and arbitrary shaped plates too.

7. REFERENCES

[1] W. Leissa: *Vibration of Plates*, Scientific and Technical Information Division, National Aeronautics and Space Administration, Columbus, 1969.

[2] Z. Su & L. Ye*: Fundamentals and Analysis of Lamb Waves. In: Identification of Damage Using Lamb Waves: From Fundamentals to Applications*, Springer London, London, 2009.

[3] J.D. Lord and R. Morrell: "Elastic Modulus Measurement, A National Measurement Good Practice Guide," DTI, National Physics Laboratory, Teddington, 2006.

[4] M. Alfano and L. Pagnotta: "Determining the elastic constants of isotropic materials by modal vibration testing of rectangular thin plates," *Journal of Sound and Vibration*, Vol. 293, No. 1–2, pp. 426–439, 2006.

[5] R. Gopikrishna, M. P. Amani, and M. Varadanam: "Evaluation of elastic modulus of metals using Acoustic Emission technique," *Proc. of the 8th International Symp. on NDT in Aerospace*, 2016.

[6] M. Miller, S. Malakooti, T. Taghvaee, N. Xiang, H. Lu, and N. Leventis: "Bending wave based characterization of viscoelastic materials," *Proc. of the 23rd International Congress on Acoustics*, No. 1, pp. 1318–1322.

[7] ASTM, E1876-09: Standard Test Method for Dynamic Young's Modulus, Shear Modulus, and Poisson's Ratio by Impulse Excitation of Vibration, United States, 2009.

[8] J. G. McDaniel, P. Dupont and L. Salvino: "A wave approach to estimating frequency-dependent damping under transient loading," *Journal of Sound and Vibration*, Vol. 231, pp. 433–449, 2000.

[9] N. Ferguson, C. Halkyard, B. Mace and K. Heron: "The estimation of wavenumbers in two-dimensional structures," *Proc. of ISMA 2002*, pp.799–806, 2002.

[10] R. Cherif and N. Atalla: "Experimental investigation of the accuracy of a vibroacoustic model for sandwich-composite panels," *Journal of Acoustical Society of America*, Vol. 137, No. 3, pp. 1541–50, 2015.

[11] A. Zerwer M. A. Polak and J. C. Santamarina: "Wave propagation in thin Plexiglas plates: implications for Rayleigh waves," NDT E Int,, Vol. 33, No. 1, pp. 33–41, 2000.

[12] J. Berthaut, M. N. Ichchou and L. Jezequel: "K-space identification of apparent structural behaviour," Journal of Sound and Vibration, Vol. 280, pp. 1125-1131, 2005.

[13] R. Cherif, J. D. Chazot and N. Atalla: "Damping loss factor estimation of two-dimensional orthotropic structures from a displacement field measurement," Journal of Sound and Vibration, Vol. 356, pp. 61-71, 2015.

[14] N. B. Roozen, Q. Leclère, K. Ege, Y. Gerge: "Estimation of plate material properties by means of a complex wavenumber fit using Hankel's functions and the image source method," *Journal of Sound and Vibration*, Vol. 390, pp. 257-271, 2017.

[15] P. Margerit, A. Lebée, J-F. Caron, K. Ege and X. Boutillon: "The High-Resolution Wavevector Analysis for the characterization of the dynamic response of composite plates*," Journal of Sound and Vibration*, Vol. 45, pp. 177–96, 2019.

[16] COMSOL Multiphysics, *Acoustics Module User's Guide*, 2018.